

# Merocyanine dyes: self-assembled monolayers

Geoffrey J. Ashwell,\* Gary A. N. Paxton, Anne J. Whittam, Wayne D. Tyrrel, Martial Berry and Dejian Zhou

The Nanomaterials Group, Cranfield University, Cranfield, UK MK43 0AL.  
E-mail: g.j.ashwell@cranfield.ac.uk

Received 21st November 2001, Accepted 13th February 2001  
First published as an Advance Article on the web 18th April 2002

4-{2-[N-(10-Thiododecyl)quinolinium-4-yl]vinyl}phenolate self-assembles on gold with a contact area of  $0.35 \pm 0.03 \text{ nm}^2 \text{ molecule}^{-1}$ , monolayer thickness of  $1.64 \pm 0.07 \text{ nm}$ , and dielectric permittivity components of  $\epsilon_r \approx 2.8$  and  $\epsilon_i \approx 0.6$  at 632.8 nm, which are reduced to *ca.* 2.0 and 0 respectively when exposed to an acidic medium. The films undergo a change from purple (merocyanine form) to yellow (protonated form) and, by monitoring changes in the reflectance, may be used as sensors with a detection limit of  $<1 \text{ ppm}$  for  $\text{NH}_3$  in a carrier gas. Langmuir–Blodgett (LB) films of the *N*-octadecyl analogue show similar behaviour but, for sensing applications, are disadvantaged because the phenolate group is adjacent to the substrate. They have a contact area and monolayer thickness of  $0.46 \pm 0.03 \text{ nm}^2 \text{ molecule}^{-1}$  and  $1.75 \pm 0.10 \text{ nm}$  respectively, the dimensions indicating that the molecules are either less closely packed or more tilted compared with those of the self-assembled film.

## Introduction

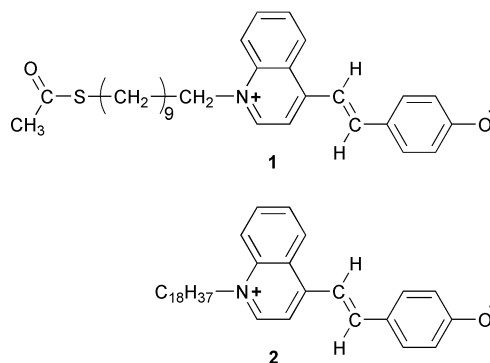
Organosulfur compounds, such as thiols, acetylthiols and disulfides,<sup>1,2</sup> self-assemble on gold and the resultant monolayers of functionalised molecules align with the groups at the surface: *e.g.*  $\text{Au-S}-(\text{CH}_2)_n\text{-A-CH=CH-D}$  for the dye described herein where A is a quinolinium acceptor and D a phenolate donor. The films are suitable for applications where a monolayer is sufficient and, in this work, we provide a comparative study of the sensing characteristics of self-assembled monolayers (SAMs) and LB films of a merocyanine. Such dyes have different absorption characteristics in acid and basic media<sup>3,4</sup> and frequently exhibit significant negative solvatochromism.<sup>4-9</sup> They are also influenced by dimeric aggregation in less polar solvents<sup>4</sup> and, as the dipole moment decreases with increasing concentration,<sup>10</sup> the molecules probably adopt a centric antiparallel arrangement in solution. This is a common feature of zwitterionic dyes and, with compact hydrophobic groups, is also adopted in LB films.<sup>11</sup> However, such molecules may be non-centrosymmetrically aligned<sup>11,12</sup> and there have been several reports of second-harmonic generation from merocyanine films<sup>13,14</sup> including multilayer structures.<sup>15</sup> Fujita *et al.*<sup>3</sup> have also described alignment *via* an Au-S-C<sub>11</sub>H<sub>22</sub> bridge, the merocyanine being a pyridinium analogue of the dye reported in this work.

We now report the synthesis of quinolinium derivatives with a 10-(acetylthio)decyl quaternary group (1) for self-assembly on gold-coated substrates and a hydrophobic octadecyl group (2) for LB deposition, their characterisation by surface plasmon resonance (SPR) and quartz crystal microbalance (QCM) studies, and an assessment of their potential use as ammonia sensors. The dyes readily protonate, both in air and at the air–water interface, and undergo a characteristic colour change from purple to yellow. The glass/Au/monolayer structures may be used as acid–base sensors by monitoring changes in the reflectance, which enables the detection of ammonia at ppm concentrations. The properties are compared as well as the relation between the SAM and LB structures.

## Experimental

Solvents and materials were obtained from the Aldrich Chemical Company and used without purification in the

synthesis of the merocyanine dyes and intermediates described below. The compounds were analysed by <sup>1</sup>H NMR, MS (FAB) and elemental techniques but the C,H,N data are excluded for 1 and 2. The dyes readily protonate in air and, unless analysed soon after purification, the data correspond to a mixture of the merocyanine form and the protonated salt.



### 1-Acetylthio-10-iododecane

1,10-Diiododecane (3.9 g, 10 mmol) and potassium thioacetate (1.1 g, 10 mmol) were refluxed in dry tetrahydrofuran (200 cm<sup>3</sup>) for 24 hours. The cooled solution was filtered to remove KI and the solvent removed by rotary evaporation. The crude product was purified by column chromatography on silica gel eluting initially with hexane and then hexane–ethyl acetate (20:1 to 50:1, v/v) to separate 1,10-diiododecane and 1,10-bis-(acetylthio)decane from the desired product. 1-Acetylthio-10-iododecane was obtained as a white solid: yield 50%; mp 27–30 °C. Found: C, 42.0; H, 6.5%. C<sub>12</sub>H<sub>23</sub>IOS requires: C, 42.11; H, 6.77%. <sup>1</sup>H NMR (CDCl<sub>3</sub>, 400 MHz, J/Hz):  $\delta_{\text{H}}$  1.28 (br s, 12 H, CH<sub>2</sub>), 1.56 (quintet, *J* 7, 2 H, CH<sub>2</sub>CH<sub>2</sub>S), 1.82 (quintet, *J* 7, 2 H, CH<sub>2</sub>CH<sub>2</sub>I), 2.32 (s, 3 H, CH<sub>3</sub>CO), 2.86 (t, *J* 7, 2 H, CH<sub>2</sub>S), 3.19 (t, *J* 7, 2 H, CH<sub>2</sub>I). MS (FAB): *m/z* 343 (100% [M + H]<sup>+</sup>).

### *N*-(10-Acetylthio)decyl-4-methylquinolinium iodide

1-Acetylthio-10-iododecane (2.0 g, 6 mmol) and 4-methylquinoline (0.86 g, 6 mmol) were refluxed in dry propan-2-ol (50 cm<sup>3</sup>) for 10 days. A yellow product was obtained by rotary evaporation

at ambient temperature. It was purified by column chromatography on silica gel, eluting with chloroform and then chloroform–methanol (10 : 1, v/v): yield, 15%; mp 91–93 °C. Found: C, 54.2; H, 6.6; N, 2.8%.  $C_{22}H_{32}INOS$  requires: C, 54.43; H, 6.64; N, 2.88%.  $^1H$  NMR ( $CDCl_3$ , 400 MHz,  $J/Hz$ ):  $\delta_H$  1.24 (br s, 8 H,  $CH_2$ ), 1.32–1.36 (m, 2 H,  $CH_2$ ), 1.45–1.54 (m, 4 H,  $CH_2$ ), 2.08 (quintet,  $J$  8, 2 H,  $CH_2CH_2N^+$ ), 2.30 (s, 3 H,  $CH_3CO$ ), 2.83 (t,  $J$  7, 2 H,  $SCH_2$ ), 3.00 (s, 3 H,  $CH_3$ ), 5.24 (t,  $J$  8, 2 H,  $CH_2N^+$ ), 7.97 (t,  $J$  8, 1 H, Qn-H), 8.00 (d,  $J$  7, 1 H, Qn-H), 8.17 (t,  $J$  9, 1 H, Qn-H), 8.28 (d,  $J$  9, 1 H, Qn-H), 8.35 (d,  $J$  9, 1 H, Qn-H), 10.25 (d,  $J$  6, 1 H, Qn-H). MS (FAB):  $m/z$ , 359 (100% [ $M + H - I$ ] $^+$ ).

**4-{2-[*N*-(10-Acetylthiodecyl)quinolinium-4-yl]vinyl}phenolate (dye 1).** A solution of *N*-(10-acetylthiodecyl)-4-methylquinolinium iodide (0.48 g, 1 mmol), 4-hydroxybenzaldehyde (0.23 g, 1 mmol) and piperidine (0.1  $cm^3$ ) in methanol (20  $cm^3$ ) was heated at reflux for 2 h. The precipitate, obtained from the cooled solution, was purified by column chromatography on silica gel, eluting initially with chloroform and then chloroform–methanol (10 : 1 to 2 : 1, v/v). Additional purification using preparative plate chromatography yielded purple (merocyanine) and yellow (protonated) forms of the dye, which were recrystallised from methanol. The merocyanine form readily protonates in the presence of  $H^+$ .  $^1H$  NMR ( $CDCl_3 + CF_3COOD$ , 250 MHz,  $J/Hz$ ):  $\delta_H$  1.27 (br s, 10 H,  $CH_2$ ), 1.50–1.78 (m, 4 H,  $CH_2$ ), 2.08 (quintet,  $J$  8, 2 H,  $CH_2CH_2N^+$ ), 2.30 (s, 3 H,  $CH_3CO$ ), 2.89 (t,  $J$  7, 2 H,  $SCH_2$ ), 4.83 (t,  $J$  8, 2 H,  $CH_2N^+$ ), 6.99 (d,  $J$  8, 2 H, Ar-H), 7.66 (d,  $J$  9, 2 H, Ar-H), 7.85 (d,  $J$  15, 1 H, C=C-H), 7.95 (d,  $J$  7, 1 H, Qn-H), 8.00 (br m, 2 H, C=CH and Qn-H), 8.08 (t,  $J$  8, 1 H, Qn-H), 8.18 (d,  $J$  9, 1 H, Qn-H), 8.44 (d,  $J$  9, 1 H, Qn-H), 8.81 (d,  $J$  6, 1 H, Qn-H), 9.65 (s, 1 H, OH).  $m/z$  (FAB): 462 (100% [ $M + H$ ] $^+$ ).

**4-[2-(*N*-Octadecylquinolinium-4-yl)vinyl]phenolate (dye 2).** The procedure was adapted from above by using *N*-octadecyl-4-methylquinolinium iodide in place of the 10-acetylthiodecyl derivative.  $^1H$  NMR ( $CDCl_3 + CF_3COOD$ , 400 MHz,  $J/Hz$ ):  $\delta_H$  0.86 (t,  $J$  7, 3 H,  $CH_3$ ), 1.25 (br s, 26 H,  $CH_2$ ), 1.34–1.46 (m, 4 H,  $CH_2$ ), 2.07 (quintet,  $J$  7, 2 H,  $CH_2CH_2N^+$ ), 4.83 (t,  $J$  8, 2 H,  $CH_2N^+$ ), 6.96 (d,  $J$  8, 2 H, Ar-H), 7.65 (d,  $J$  9, 2 H, Ar-H), 7.74–7.81 (m, 2 H, C=C-H and Qn-H), 7.98 (t,  $J$  8, 1 H, Qn-H), 8.12–8.19 (m, 3 H, C=C-H and Qn-H), 8.62 (d,  $J$  8, 1 H, Qn-H), 8.87 (d,  $J$  6, 1 H, Qn-H), 9.87 (s, 1 H, OH).  $m/z$  (FAB): 500 (100% [ $M + H$ ] $^+$ ).

## Results and discussion

### Solution studies

The dyes exhibit negative solvatochromism, for example, from 505 nm in water to 670 nm in chloroform. This is a common feature of merocyanine dyes and is depicted in Fig. 1 as the transition energy of the high wavelength band *versus* Reichardt's normalised polarity parameter ( $E_T^N$ ).<sup>17</sup> This extreme form of solvatochromism has been attributed to the zwitterionic ground state,<sup>5–9</sup> to the hydrogen-bonding ability of the donor in protic solvents<sup>18,19</sup> and to nucleophile–carbonyl interactions in acetone.<sup>19</sup> Furthermore, although the dyes have a single symmetrical charge-transfer band in polar solvents, they exhibit multiple maxima when  $E_T^N < 0.5$ , for example, at *ca.* 570 nm (sh), 625 nm and 670 nm in chloroform. This may be explained by association<sup>4</sup> whereby the principal bands correspond to transitions of the molecule and aggregate. A Benesi–Hildebrand analysis<sup>20</sup> has not been possible in this case as the charge-transfer bands are too closely spaced. However, dimeric aggregation has been confirmed from the concentration dependence of the charge-transfer spectra of related zwitterionic dyes: for example, 4-(*N*-hexadecylquinolinium-4-ylmethylideneamino)-2,6-dichlorophenolate, its pyridinium

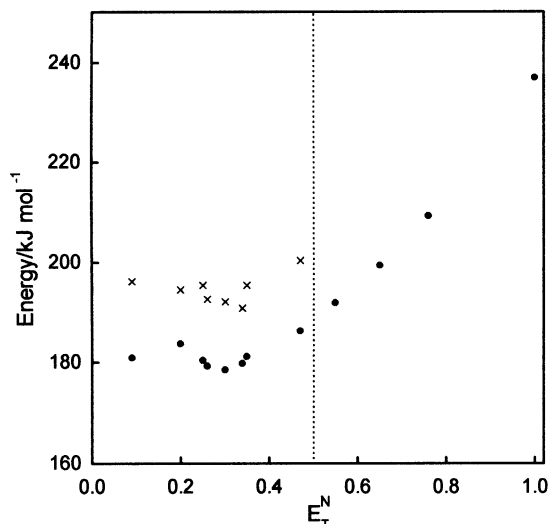


**Fig. 1** Energy of the intramolecular charge-transfer band of the dyes *versus* Reichardt's normalised solvent polarity parameter: toluene ( $E_T^N = 0.09$ ), tetrahydrofuran (0.20), ethyl acetate (0.23), chloroform (0.26), dichloromethane (0.32), benzonitrile (0.34), acetone (0.35), acetonitrile (0.47), propan-2-ol (0.55), ethanol (0.65), methanol (0.76) and water (1.00). The two analogues are insoluble in water and, thus, the value at  $E_T^N = 1.00$  relates to the *N*-butyl derivative, which exhibits identical spectra in all solvents. The dyes have a symmetrical charge-transfer band in solvents to the right of the vertical line but aggregate with multiple maxima in those to the left: ●, intramolecular transition; ×, aggregate band.

congener<sup>4</sup> and 4-{*N*-(hexadecyldiphenylphosphonio)benzylidene]amino}-2,6-dihalophenolate.<sup>21</sup> This has also been demonstrated by the mass spectra which show  $m/z$  values consistent with both the molecule and dimer.<sup>11,21</sup> It appears to be a common feature of such dyes and antiparallel coupling of D– $\pi$ –A chromophores has been reported from the concentration dependence of the dipole moment.<sup>10</sup>

### SAMs

Dye 1 was chemisorbed on gold-coated substrates by immersion in a  $5 \times 10^{-4}$  M ethanol solution containing ammonium hydroxide to remove the acetyl group, the substrates being thoroughly rinsed with ethanol to remove any physisorbed material and dried in warm air. Self-assembly on 10 MHz quartz crystals provided the mass and, thus, the molecular area in contact with the central gold electrodes. Progress was monitored by the frequency change and the area derived from the Sauerbrey equation:<sup>22</sup>

$$\text{Area} = -4F_o^2 m / \Delta F (\rho \mu)^{1/2} \quad (1)$$

The terms are defined as follows:  $F_o$ , resonance frequency;  $\Delta F$ , frequency change;  $\rho$ , density of quartz (2.648 Mg  $m^{-3}$ );  $\mu$ , shear modulus ( $2.947 \times 10^7$  Mg  $m^{-1} s^{-2}$ );  $m$ , mass of the surface-bound molecule where  $m = ML^{-1}$  and  $M$  and  $L$  are the molecular mass and Avogadro's constant respectively. The area decreased to a constant value of  $0.35 \pm 0.03$  nm<sup>2</sup> molecule<sup>-1</sup>, which is only slightly greater than the van der Waals cross-section of the quinolinium group (*cf.* 0.29 nm<sup>2</sup>). Thus, allowing for molecular tilt, the data indicate that the molecules are densely packed but the estimated area is only valid for chemisorbed dye and may be influenced by physisorbed material.

Self-assembly of the thio derivative on BK7 glass, with a 45 nm thick gold overlay, and subsequent investigation of the SPR data provided the monolayer thickness and dielectric permittivities. SPR studies were performed on glass/Au/SAM structures using a Kretschmann geometry<sup>23</sup> and p-polarised monochromatic light at the following wavelengths: 532 and

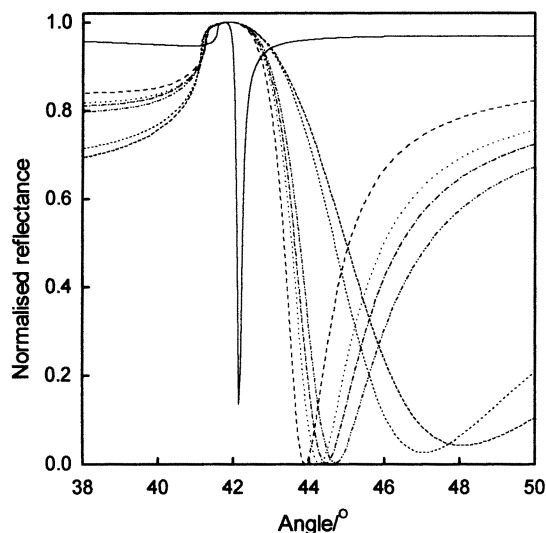


**Fig. 2** SPR spectra of a glass/Au/SAM structure of dye **1** on a  $40.6 \pm 0.2$  nm thick gold overlay at the following excitatory wavelengths: 532 and 1064 nm (Nd:YAG); 543.5, 594.1, 604.0, 611.9 and 632.8 nm (HeNe). The spectrum broadens and the resonance angle increases with decreasing wavelength. The organic monolayer has a thickness of  $1.64 \pm 0.07$  nm and dielectric permittivities of  $\epsilon_r \approx 2.5$  and  $\epsilon_i \approx 0.2$  at 532 nm which increase to  $\epsilon_r \approx 2.8$  and  $\epsilon_i \approx 0.6$  at 632.8 nm. For clarity, the 250 data points per scan are excluded but, in each case, they directly overlap the theoretical fit.

1064 nm (Nd:YAG) and 543.5, 594.1, 604.0, 611.9 and 632.8 nm (multiline HeNe laser). The attenuated total reflection was measured before and after deposition and the data analysed by one and two-layer models respectively using Fresnel reflection formulae. Data for the seven excitatory wavelengths shown in Fig. 2 yielded a mean thickness of  $1.64 \pm 0.07$  nm for the monolayer, which together with the contact area and molecular mass, provided a density  $1.2 \pm 0.2$  Mg m<sup>-3</sup>. The real and imaginary components of the dielectric permittivity are typically  $\epsilon_r \approx 2.8$  and  $\epsilon_i \approx 0.6$  at 632.8 nm but, as the dye readily protonates in air, the values may be influenced by the coexistence of the yellow hydroxy form which is transparent above 600 nm. The resonant angle is shifted to higher values when the film is exposed to ammonia and to lower values when exposed to acid but analysis of the films, post exposure, has not provided reliable data from the fitting routine. Nonetheless, the protonated films are suitable as ammonia sensors with the concentration monitored by utilising changes in the SPR reflectance at a fixed angle of incidence.

For comparison, self-assembled films of the intermediates, 1-acetylthio-10-iododecane and *N*-(10-acetylthiododecyl)-4-methylquinolinium iodide, were similarly obtained by immersing gold-coated substrates in ethanol solutions containing ammonium hydroxide to remove the acetyl group. The areas in contact with the substrate, obtained by analysis of the QCM data, decreased to a constant value of *ca.*  $0.6$  nm<sup>2</sup> molecule<sup>-1</sup> in each case. Furthermore, analysis of the SPR data from glass/Au/SAM structures of the quinolinium salt, fabricated under identical conditions, gave a monolayer thickness of 1.82 nm (*cf.* 2.0 nm molecular length). These dimensions suggest that the molecules are far less closely packed than in films of the dye, which adopts a tilted arrangement probably arising from charge-transfer interactions between the donor and acceptor groups of neighbouring molecules.

#### Langmuir and LB films

The merocyanine form of **2** was spread from a  $2 \times 10^{-4}$  M chloroform solution onto the pure water subphase of a Langmuir trough (Nima Technology, model 611) with a sapphire window in the base. The film was left for 10 min at

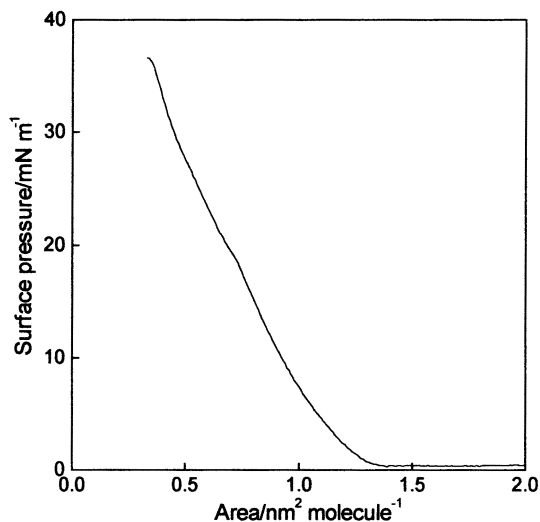


**Fig. 3** Surface pressure *versus* area isotherms of **2**. Areas were calculated using the molecular mass of the merocyanine form but, as the dye readily protonates in air, the actual area may be larger than indicated.

20 °C and then compressed at  $0.5$  cm<sup>2</sup> s<sup>-1</sup>, which corresponded to a rate of *ca.*  $0.1\%$  s<sup>-1</sup> of the compartment area. The surface pressure *versus* area isotherm is generally featureless, there being a slight inflection at *ca.*  $18$  mN m<sup>-1</sup> and collapse at *ca.*  $36$  mN m<sup>-1</sup> (Fig. 3). The molecular footprint in the high-pressure regime indicates that the chromophores are vertically aligned and, therefore, dimeric aggregates that may exist in the spreading solution disintegrate at the air–water subphase. A limiting area corresponding to the chromophore edge would be anticipated if an antiparallel arrangement were maintained, the likely configuration being U-shaped with both alkyl groups pointing upwards.

The visible spectrum of the floating monolayer, obtained in transmission using an Instaspec fibre-optic CDD spectrometer, is dependent upon the pH of the aqueous subphase. The dye readily protonates, even when spread on freshly purified water, and its spectrum shows a coexistence of both forms (Fig. 4). The absorption band of the protonated form is centred about 440 nm whereas, when the dye is spread on a basic subphase, the transition is red-shifted to 580 nm and this conforms to the merocyanine (Fig. 5).

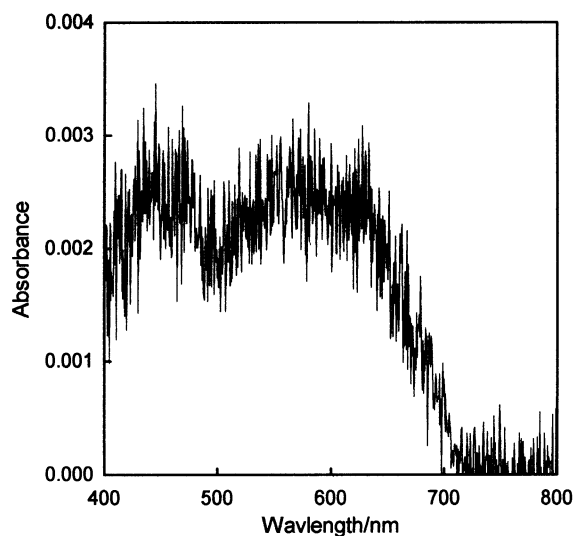


**Fig. 4** Visible spectrum of a floating monolayer of dye **2** at  $30$  mN m<sup>-1</sup> on an ultrapure aqueous subphase (MilliQ), the water being freshly purified. The broad spectrum corresponds to protonated and merocyanine forms of the dye.

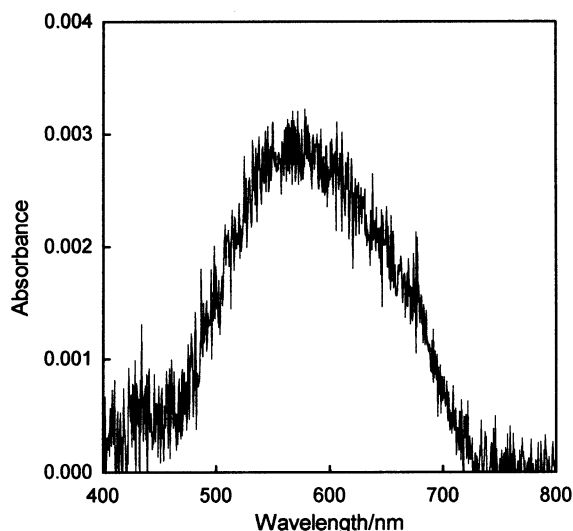


**Fig. 5** Visible spectrum of a floating monolayer of **2** at  $30 \text{ mN m}^{-1}$  on an aqueous subphase at pH 10, the absorption band corresponding to the merocyanine form only. The protonated form has an absorption maximum at 440 nm with cut-off above 600 nm.

Films were deposited using a model 622 Nima Technology LB trough. They were transferred on the upstroke by passing substrates, 10 MHz quartz crystals and gold-coated BK7 glass, through the floating monolayer at a rate of  $30 \mu\text{m s}^{-1}$  with the film compressed to  $30 \text{ mN m}^{-1}$ . SPR studies were performed on glass/Au/monolayer structures using a Kretschmann configuration<sup>23</sup> and an excitatory wavelength of 632.8 nm. Analysis of the experimental data shown in Fig. 6, using a two-layer model, gave a monolayer thickness of  $1.75 \pm 0.10 \text{ nm}$  and real and imaginary components of the dielectric permittivity of  $\epsilon_r \approx 2.1$  and  $\epsilon_i \approx 0.1$  respectively. The low values indicate protonation at the air–water interface but, when the film is exposed to ammonia vapour, they increase to  $\epsilon_r \approx 3.0$  and  $\epsilon_i \approx 0.6$ . The values reflect the extremes of the range observed for both the SAM and LB film.

A Sauerbrey analysis<sup>22</sup> of the frequency change of an AT-cut 10 MHz quartz crystal, upon deposition of an LB monolayer, provided a molecular footprint of  $0.46 \pm 0.03 \text{ nm}^2 \text{ molecule}^{-1}$

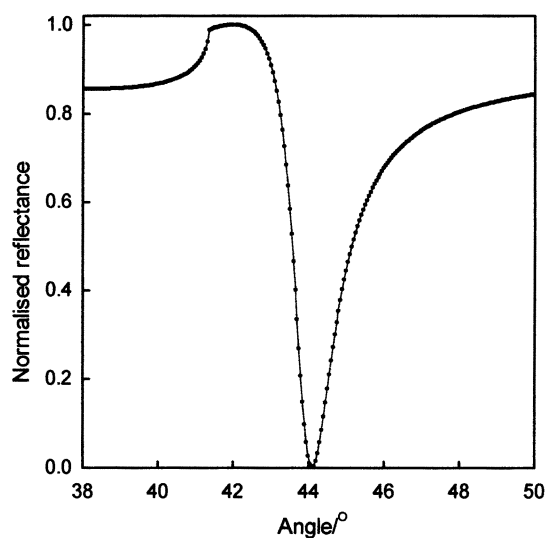


**Fig. 6** SPR spectrum of a glass/Au/LB structure of dye **2** at an excitatory wavelength of 632.8 nm. The gold overlay has a thickness of  $47.2 \pm 0.1 \text{ nm}$  and real and imaginary components of the dielectric permittivity of  $\epsilon_r = -11.4 \pm 0.1$  and  $\epsilon_i = 1.2 \pm 0.1$  respectively. Corresponding data for the organic monolayer are  $d = 1.75 \pm 0.10 \text{ nm}$ ,  $\epsilon_r \approx 2.1$  and  $\epsilon_i \approx 0.1$ , the permittivities being significantly reduced by protonation of the dye at the air–water interface.

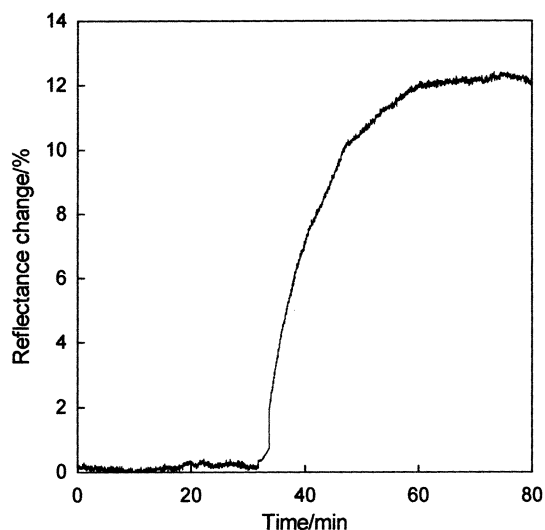


**Fig. 7** Variation of the reflectance change from a glass/Au/monolayer structure of the protonated form when exposed to 100 ppm  $\text{NH}_3$  in nitrogen at *ca.*  $-0.4^\circ$  from the resonant angle. The percentage change is dependent upon the angle of incidence of the laser beam but is approximately linear with the concentration of gas and the device has a detection limit of *ca.* 1 ppm. Reversal occurs when exposed to an acidified carrier gas.

in contact with the substrate. This suggests that the chromophores are less densely packed in the LB film than in the SAM (*cf.*  $0.35 \pm 0.03 \text{ nm}^2 \text{ molecule}^{-1}$ ) and this may be attributed, in part, to pinholes and, in part, to the larger hydrophobic groups which tend to have lower packing densities. However, the areas may also be explained by different molecular tilts.

### Sensing

The protonated form is transparent at the red end of the spectrum (cut-off,  $\lambda > 600 \text{ nm}$ ) whereas the merocyanine form is absorbing. Consequently, large differences in the dielectric permittivities render the SPR technique sensitive for detection with inexpensive laser diodes. Typical changes in the normalised reflectance of the protonated form, upon exposure to 100 ppm of  $\text{NH}_3$ , are shown in Fig. 7 for an excitatory wavelength of 632.8 nm. The data indicate 25 min to equilibrium and *ca.* 6 min to 50% equilibrium ( $t_{1/2}$ ). However, our studies indicate a range of behaviour with  $t_{1/2} < 1 \text{ min}$ . Such differences are attributed to film quality and for LB films, where the phenolate group is adjacent to the substrate, to the difficulty of diffusion in nonporous structures. The SPR response of LB films is also affected by the ammonium salt, which becomes trapped and results in the film becoming cloudy after a few cycles. However, this does not apply to SAM structures where the phenolate group is at the surface. These have a detection limit of *ca.* 1 ppm  $\text{NH}_3$  in nitrogen at 632.8 nm.

### Acknowledgement

One of us (G.J.A.) is grateful to the EPSRC UK for funding this work and acknowledges Dan Portus and Mike Roberts for technical assistance. The EPSRC is also acknowledged for providing PhD studentship support to G.A.N.P., W.T. and M.B.

### References

- 1 F. Schreiber, *Progr. Surf. Sci.*, 2000, **65**, 151.
- 2 J. M. Tour, L. Jones, D. L. Pearson, J. J. S. Lamba, T. P. Burgin, G. M. Whitesides, D. L. Allara, A. N. Parikh and S. V. Atre, *J. Am. Chem. Soc.*, 1995, **117**, 9529.

- 3 K. Fujta, M. Hara, H. Sasabe, W. Knoll, K. Tsuboi, K. Kajikawa, K. Seki and Y. Ouchi, *Langmuir*, 1998, **14**, 7456.
- 4 G. J. Ashwell, K. Skjonnemand, G. A. N. Paxton, D. W. Allen, J. P. L. Mifflin and X. Li, *J. Mater. Chem.*, 2001, **11**, 1351.
- 5 S. Rajagopal and E. Buncel, *Dyes and Pigments*, 1991, **17**, 303.
- 6 S. Arai, H. Arai, M. Hida and T. Yamagishi, *Heterocycles*, 1994, **38**, 2449.
- 7 C. Machado, M. de G. Nascimento and M. C. Rezende, *J. Chem. Soc., Perkin Trans. 2*, 1994, 2539; L. Dasilva, C. Machado and M. C. Rezende, *J. Chem. Soc., Perkin Trans. 2*, 1995, 483.
- 8 D. W. Allen and X. Li, *J. Chem. Soc., Perkin Trans. 2*, 1997, 1099.
- 9 C. Reichardt, S. Lobbecke, A. M. Mehranpour and G. Schafer, *Can. J. Chem.*, 1998, **76**, 686.
- 10 F. Würthner and S. Yao, *Angew Chem., Int. Ed.*, 2000, **39**, 1978.
- 11 G. J. Ashwell and G. A. N. Paxton, *Aust. J. Chem.*, in press.
- 12 G. J. Ashwell, G. Jefferies, E. J. C. Dawnay, A. P. Kuczynski, D. E. Lynch, G. Yu and D. G. Bucknall, *J. Mater. Chem.*, 1995, **5**, 975.
- 13 I. R. Girling, N. A. Cade and C. M. Montgomery, *Electron. Lett.*, 1985, **21**, 169.
- 14 L. M. Hayden, S. T. Kowel and M. P. Srinivasan, *Opt. Commun.*, 1987, **61**, 289.
- 15 R. H. Tredgold, M. C. J. Young, R. Jones, P. Hoge, P. Kolinski and R. J. Jones, *Electron. Lett.*, 1988, **24**, 308.
- 16 D. I. Gittins, D. Bethell, R. J. Nicholls and D. J. Schiffrin, *J. Mater. Chem.*, 2000, **10**, 79.
- 17 C. Reichardt, *Solvents and Solvent Effects in Organic Chemistry*, 2nd edn. VCH, Weinheim, 1988.
- 18 E. Hamman and A. M. El-Nahas, *J. Phys. Chem. A*, 1998, **102**, 9739.
- 19 S. F. Alberti and J. Echave, *Chem. Phys.*, 1997, **223**, 183.
- 20 H. A. Benesi and J. H. Hildebrand, *J. Am. Chem. Soc.*, 1949, **71**, 2703.
- 21 D. W. Allen, M. R. Clench, J. P. L. Mifflin, A. J. Whittam and G. J. Ashwell, *J. Mater. Chem.*, to be submitted.
- 22 G. Sauerbrey, *Z. Phys.*, 1959, **155**, 206.
- 23 E. Kretschmann, *Z. Phys.*, 1971, **241**, 313.